*Inorg. Chem.* **2007**, *46*, 10461–10463

# Field-Induced Metamagnetic Transition in the $Fe^{III}$–$Mn^{III}$ Bimetallic Chain Built by a New Cyanide-Bearing $Fe^{III}$ Precursor

**Jae Il Kim,[†] Houng Sik Yoo,[†] Eui Kwan Koh,[‡] and Chang Seop Hong*[,†]**

*Department of Chemistry, Korea University, Seoul 136-713, Korea, and Nano-Bio System Research Team, Korea Basic Science Institute, Seoul 136-713, Korea*

Received October 10, 2007

The use of a new precursor, *mer*-$[Fe(mpzcq)(CN)_3]^-$ (**1**), produced a dimeric molecule, $[Fe(mpzcq)(CN)_3][Mn(salen)(H_2O)]\cdot H_2O$ (**2**), and a one-dimensional zigzag chain, $[Fe(mpzcq)(CN)_3][Mn(salcy)]\cdot MeOH\cdot MeCN$ (**3**). Antiferromagnetic couplings are operating between magnetic centers through CN ligands, and a field-induced metamagnetic transition is observed in **3**.

The capped molecular precursors $[Fe(L)(CN)_x]^{y-}$ (L = blocking ligands; $x = 2-5$), where $Fe^{III}$ can act as an anisotropic center, have been utilized in the construction of magnetically interesting systems with *n*-dimensional structures ($n = 0$ and 1).[1] The existence of the ancillary ligand in the precursors plays a key role in controlling the directions of structural propagation, which helps to create low-dimensional materials. In the case of L = tridentate ligand and $x = 3$, facial and meridional isomers are present, depending on the arrangement of three cyanide groups around the coordination sphere. Most of the studies in the field of molecular magnetism are focused on facial iron(III) tricyanide precursors.[2] In contrast, only a few $Mn^{II}-Fe^{III}$ bimetallic assemblies containing *mer*-$[Fe(L)(CN)_3]^-$ [L = bis(2-pyridylcarbonyl)amidate anion or 8-(pyridine-2-carboxamido)-quinoline anion] were reported.[3,4] Recently, we explored the $Mn^{III}-Fe^{III}$ system in search of magnetically anisotropic entities by employing the new *mer*-iron tricyanide building unit.[5] To gain insight into the magnetic exchange occurring in the series, more examples involving *mer*-iron tricyanide are sought.

Herein we report the synthesis, structures, and magnetic properties of a new molecular building unit, $(PPh_4)[Fe(mpzcq)(CN)_3]$ [**1**; mpzcq = 8-(5-methylpyrazine-2-carboxamido)quinoline anion], a dimeric molecule, $[Fe(mpzcq)(CN)_3][Mn(salen)(H_2O)]\cdot H_2O$ [**2**; salen = *N*,*N*′-ethylenebis(salicylideneiminato) dianion], and a one-dimensional zigzag chain, $[Fe(mpzcq)(CN)_3][Mn(salcy)]\cdot MeOH\cdot MeCN$ [**3**; salcy = *N*,*N*′-(*trans*-1,2-cyclohexanediylethylene)bis-(salicylideneiminato) dianion] (Figure 1). It is worth noting that **3** is the first example of the cyanide-bridged $Fe^{III}-Mn^{III}$ ferrimagnetic chains exhibiting a metamagnetic transition, fabricated by the *mer*-iron(III) cyanide and the manganese-(III) Schiff base.[3−5]

A stoichiometric reaction of $[Fe(mpzcq)(CN)_3]^-$ and the corresponding manganese Schiff bases in a mixed solvent of $MeOH/MeCN/H_2O$ afforded brown crystals of dimeric **2** and one-dimensional **3**.[6] The anionic building unit, *mer*-$[Fe(mpzcq)(CN)_3]^-$, can be readily incorporated into the bimetallic complexes by self-assembling with cationic manganese Schiff bases. The use of the precursor chelated with mpzcq produced the Fe−Mn(salen) dimer, which is compared with the one-dimensional $Fe^{III}-Mn^{III}$ system isolated in the presence of *mer*-$[Fe(pzcq)(CN)_3]^-$ and $Mn(salen)^+$, where pzcq is less bulky than mpzcq.[5] The steric consequence of mpzcq really affects the structural pattern as in this case. The same type of a zigzag $Fe^{III}-Mn^{III}$ chain could be

* To whom correspondence should be addressed. E-mail: cshong@korea.ac.kr.
[†] Korea University.
[‡] Korea Basic Science Institute.

(1) (a) Toma, L. M.; Lescouëzec, R.; Lloret, F.; Julve, M.; Vaissermann, J.; Verdaguer, M. *Chem. Commun*, **2003**, 1850. (b) Lescouëzec, R.; Vaissermann, J.; Ruiz-Pérez, C.; Lloret, F.; Carrasco, R.; Julve, M.; Verdaguer, M.; Dromzee, Y.; Gatteschi, D.; Wernsdorfer, W. *Angew. Chem., Int. Ed.* **2003**, *42*, 1483. (c) Toma, L. M.; Lescouëzec, R.; Pasán, J.; Ruiz-Pérez, C.; Vaissermann, J.; Cano, J.; Carrasco, R.; Wernsdorfer, W.; Lloret, F.; Julve, M. *J. Am. Chem. Soc.* **2006**, *128*, 4842. (d) Ni, Z.-H.; Kou, H.-Z.; Zhao, Y.-H.; Zheng, L.; Wang, R.-J.; Cui, A.-L.; Sato, O. *Inorg. Chem.* **2005**, *44*, 2050. (e) Ni, W.-W.; Ni, Z.-H.; Cui, A.-L.; Liang, X.; Kou, H.-Z. *Inorg. Chem.* **2007**, *46*, 22.

(2) (a) Liu, W.; Wang, C.-F.; Li, Y.-Z.; Zuo, J.-L.; You, X.-Z. *Inorg. Chem.* **2006**, *45*, 10058. (b) Wen, H.-R.; Wang, C.-F.; Song, Y.; Gao, S.; Zuo, J.-L.; You, X.-Z. *Inorg. Chem.* **2006**, *45*, 8942. (c) Gu, Z.-G.; Yang, Q.-F.; Liu, W.; Song, Y.; Li, T.-Z.; Zuo, J.-L.; You, X.-Z. *Inorg. Chem.* **2006**, *45*, 8895. (d) Wang, S.; Zuo, J.-L.; Zhou, H.-C.; Choi, H. J.; Ke, Y.; Long, J. R.; You, X.-Z. *Angew. Chem., Int. Ed.* **2004**, *43*, 5940. (e) Li, D.; Parkin, S.; Wang, G.; Yee, G. T.; Prosvirin, A. V.; Holmes, S. M. *Inorg. Chem.* **2005**, *44*, 4903. (f) Li, D.; Parkin, S.; Wang, G.; Yee, G. T.; Clérac, R.; Wernsdorfer, W.; Holmes, S. M. *J. Am. Chem. Soc.* **2006**, *128*, 4214. (g) Yang, J. Y.; Shores, M. P.; Sokol, J. J.; Long, J. R. *Inorg. Chem.* **2003**, *42*, 1403. (h) Wang, S.; Zuo, J.-L.; Gao, S.; Song, Y.; Zhuo, H.-C.; Zhang, Y.-Z.; You, X.-Z. *J. Am. Chem. Soc.* **2004**, *126*, 8900.

(3) Lescouëzec, R.; Vaissermann, J.; Toma, L. M.; Carrasco, R.; Lloret, F.; Julve, M. *Inorg. Chem.* **2004**, *43*, 2234.

(4) Ni, Z.-H.; Kou, H.-Z.; Zhang, L.-F.; Ni, W.-W.; Jiang, Y.-B.; Cui, A.-L.; Ribas, J.; Sato, O. *Inorg. Chem.* **2005**, *44*, 9631.

(5) Kim, J. I.; Yoo, H. S.; Koh, E. K.; Kim, H. C.; Hong, C. S. *Inorg. Chem.* **2007**, *46*, 8481.

(6) See the Supporting Information.

10.1021/ic702001q CCC: $37.00 
Published on Web 11/15/2007

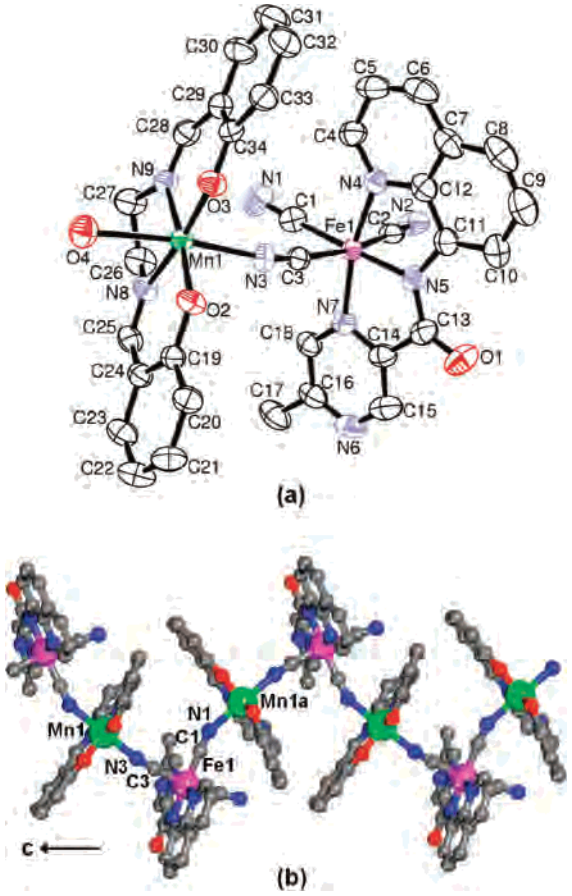


**Figure 1.** Molecular views of (a) **2** and (b) **3** showing the atom-labeling scheme. Symmetry code: a = *x*, 0.5 − *y*, 0.5 + *z*.

achieved when one utilized the $Mn(salcy)^+$ moiety as a counterpart. In the IR spectra, the characteristic CN peaks are positioned at 2127m (sh) and 2114m $cm^{-1}$ for **1**, 2121m and 2114m $cm^{-1}$ for $K[Fe(mpzcq)(CN)_3]$, 2139m, 2127m, and 2116m $cm^{-1}$ for **2**, and 2131m and 2119m $cm^{-1}$ for **3**. When compared with the precursor, the peak shift toward higher frequencies suggests the presence of bridging CN ligands.

All compounds crystallize in the monoclinic system, as analyzed by X-ray crystallography (Figure S1 in the Supporting Information).[7] Each central iron environment can be described as distorted octahedral, comprising three C atoms from terminal CN ligands and three N atoms from the tridentate ligand mpzcq. The Fe−C(cyanide) bond lengths span from 1.940 to 1.964 Å for **1**, from 1.948 to 1.955 Å for **2**, and from 1.938 to 1.961 Å for **3**, which tend to be reduced when the coordination of cyanides to the $Mn^{III}$ centers is formed. The shorter Fe−N(amide) bond distances [1.893(2) Å for **1**, 1.894(2) Å for **2**, and 1.882(4) Å for **3**] than the other Fe−N lengths in the range of 1.950−1.983 Å are associated with a strong $\sigma$-donor effect of the deprotonated amide.[3−5] The maximum deviation of the Fe−C−N angle from linearity is 3.5° for **1**, 7.4° for **2**, and 4.1° for **3**. For the manganese Schiff base fragment, the $MnN_2O_2$ moiety generated from the Schiff base ligand forms the equatorial plane [ave Mn−N(O) = 1.93(7) Å for **2** and 1.94(6) Å for **3**], while the apical positions are taken by two N(O) atoms from bridging cyanides or a terminal water molecule [Mn1−N3 = 2.275(3) Å and Mn1−O4 = 2.391(2) Å for **2** and Mn1−N3 = 2.287(5) Å and Mn1−N1b = 2.298(5) Å for **3**; b = *x*, 0.5 − *y*, −0.5 + *z*]. These tetragonal elongations are typical of the Jahn−Teller distortion around an octahedral $Mn^{III}$ ion.[8] The important angles in the bridging pathways are found at 164.1(2)° for Mn1−N3−C3 (**2**) and 169.1(4)° for Mn1−N3−C3 and 154.3(5)° for Mn1a−N1−C1 (**3**; a = *x*, 0.5 − *y*, 0.5 + *z*). These values are larger than the cyanide-bridged Fe−Mn chain with pzcq.[5] The intrachain Fe−Mn distances through the CN bridges are 5.2902(8) Å for Fe1−Mn1 (**2**) and 5.3793(11) Å for Fe1−Mn1 and 5.2348(10) Å for Fe1−Mn1a (**3**). The dihedral angle between the $MnN_2O_2$ basal planes within a chain for **3** corresponds to 75.29(9)°, which is greater than that [69.41(6)°] of the Fe−Mn system with pzcq.[5]

In the extended structure of **2**, the dimeric units are linked by $\pi-\pi$ interactions between aromatic rings of salen and mpzcq, leading to a three-dimensional architecture (Figure S2 in the Supporting Information). The O5 atom of a lattice water molecule is simultaneously hydrogen-bonded to two N atoms (N1 and N2) from unbound CN ligands [O5−N1 = 2.881(5) Å; O5−N2 = 2.910(4) Å] and one O atom (O4) from a coordinated water molecule [O5−O2 = 2.791(4) Å]. The shortest interdimer metal−metal distance is found to be 6.716(1) Å for Fe1−Mn1. For **3**, $\pi-\pi$ stackings occur between the whole quinoline subunits of mpzcq ligands with an interchain Fe−Fe distance of 8.813(1) Å. It is noted that the noncovalent contacts in **3** are much more extensive than those in the Fe−Mn chain chelated with pzcq (Figure S3 in the Supporting Information). The shortest metal−metal separation between chains is 7.476(1) Å for Fe1−Fe1.

The cryomagnetic data of **2** and **3** were collected at 1000 G, as displayed in Figures S4 in the Supporting Information and 2, respectively. At 300 K, the $\chi_m T$ values are 3.49 $cm^3$ K $mol^{-1}$ (**2**) and 3.27 $cm^3$ K $mol^{-1}$ (**3**), which are close to the spin-only one (3.38 $cm^3$ K $mol^{-1}$) expected for noncoupled $Fe^{III}$ ($S_{Fe} = {}^1/_2$) and $Mn^{III}$ spins ($S_{Mn} = 2$). Both complexes undergo a gradual reduction of $\chi_m T$ as the temperature is lowered, indicating the presence of antiferromagnetic couplings between the magnetic neighbors. For **2**, a shoulder at 1.82 $cm^3$ K $mol^{-1}$ is observed around 10 K, consistent with the theoretical value (1.88 $cm^3$ K $mol^{-1}$) calculated from $S = S_{Mn} - S_{Fe} = {}^3/_2$. Below this temperature,

(7) Crystal data for **1**: $C_{42}H_{31}FeN_7OP$, $M_r$ = 736.56, monoclinic, space group *C*2/*c*, *a* = 37.6511(10) Å, *b* = 9.2841(3) Å, *c* = 27.9437(9) Å, $\beta$ = 122.201(2)°, *V* = 8265.4(4) Å$^3$, *Z* = 8, $\rho_{calcd}$ = 1.184 g $cm^{-3}$, $\mu$ = 0.443 $mm^{-1}$, *T* = 130 K, 67 045 reflections collected, 10 274 unique ($R_{int}$ = 0.1152), R1 = 0.0579, wR2 = 0.1057 [$I > 2\sigma(I)$]. Crystal data for **2**: $C_{34}H_{29}FeMnN_9O_5$, $M_r$ = 754.45, monoclinic, space group *C*/*c*, *a* = 10.7664(11) Å, *b* = 23.771(2) Å, *c* = 13.8319(15) Å, $\beta$ = 110.576(6)°, *V* = 3314.2(6) Å$^3$, *Z* = 4, $\rho_{calcd}$ = 1.512 g $cm^{-3}$, $\mu$ = 0.876 $mm^{-1}$, *T* = 293 K, 16 137 reflections collected, 7303 unique ($R_{int}$ = 0.0252), R1 = 0.0331, wR2 = 0.0841 [$I > 2\sigma(I)$]. Crystal data for **3**: $C_{41}H_{38}FeMnN_{10}O_4$, $M_r$ = 845.60, monoclinic, space group $P2_1/c$, *a* = 12.4857(4) Å, *b* = 20.3444(6) Å, *c* = 14.9471(5) Å, $\beta$ = 92.218(2)°, *V* = 3793.9(2) Å$^3$, *Z* = 4, $\rho_{calcd}$ = 1.480 g $cm^{-3}$, $\mu$ = 0.773 $mm^{-1}$, *T* = 130 K, 28 261 reflections collected, 9268 unique ($R_{int}$ = 0.0767), R1 = 0.0785, wR2 = 0.2056 [$I > 2\sigma(I)$].

(8) (a) Ko, H. H.; Lim, J. H.; Kim, H. C.; Hong, C. S. *Inorg. Chem.* **2006**, *45*, 8847. (b) Ko, H. H.; Lim, J. H.; Yoo, H. S.; Kang, J. S.; Kim, H. C.; Koh, E. K.; Hong, C. S. *Dalton Trans.* **2007**, 2061.

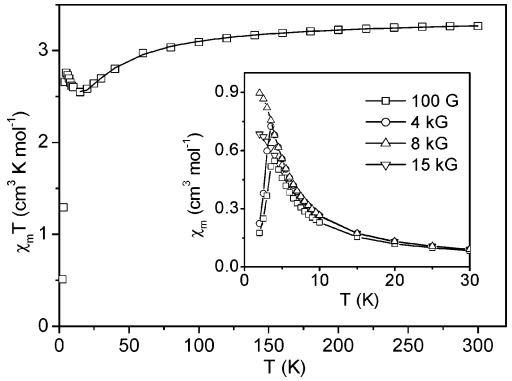


**Figure 2.** Plot of $\chi_m T$ vs $T$ of **3** at 1000 G. The solid line represents the best fit to the magnetic model. The inset shows the temperature dependence of field-cooled magnetic susceptibilities at indicated fields. The solid lines are guides to the eyes.

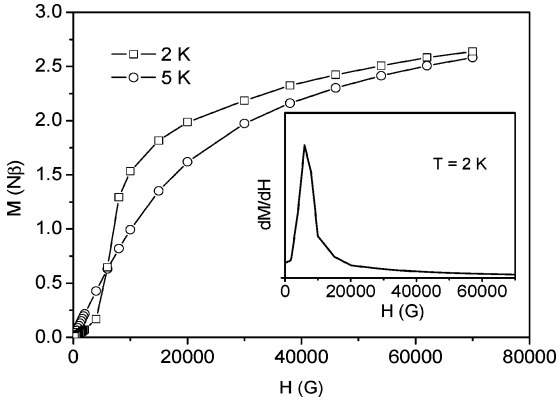


**Figure 3.** Plots of the magnetization ($M$) vs $H$ of **3** at 2 and 5 K. The inset shows the derivative of $M$ at 2 K against $H$. The peak is observed at 6 kG.

$\chi_m T$ further decreases because of interdimer antiferromagnetic interactions through the noncovalent forces. For **3**, $\chi_m T$ reaches a minimum of 2.55 cm$^3$ K mol$^{-1}$ at 15 K, increases up to 2.76 cm$^3$ K mol$^{-1}$ at 5 K, and then below the cusp temperature, it decreases again. The appearance of the valley at 15 K in the $\chi_m T$ plot is typical of a ferrimagnetic behavior.[9] The antiferromagnetic ordering occurs at 4 K, taken from the maximum of $\chi_m(T)$ at 100 G. The Curie−Weiss fits at the high-temperature ranges ($T$ > 25 K for **2** and $T$ > 30 K for **3**) give Weiss constants of −16.6 K (**2**) and −8.0 K (**3**), demonstrating the presence of antiferromagnetic alignments between spin centers.

To obtain the exchange-coupling constant in **2**, we adopted a dimer model based on the spin Hamiltonian $H = -JS_{Mn}\cdot S_{Fe}$. The molecular-field approximation was taken into consideration to account for the intermolecular magnetic interactions. The magnetic parameters are $g = 2.08$, $J = -17.2$ cm$^{-1}$, and $zJ' = -0.62$ cm$^{-1}$. The inclusion of the zero-field-splitting term ($D$) in the fitting process did not improve the result. The $M(H)$ data at 2 K affirm the antiferromagnetic nature.

To probe the magnetic nature of **3**, we employed an analytical expression derived by Drillon et al. only in the temperature range 15−300 K to preclude interchain interaction and the zero-field-splitting effect.[10] The obtained parameters are roughly estimated to be $g_{Mn} = 1.98$, $g_{Fe} = 2.08$, and $J = -6.5$ cm$^{-1}$. This confirms the presence of antiferromagnetic interactions between Mn$^{III}$ and Fe$^{III}$ ions transmitted by the bridging cyanides, which is still a rare case among cyanide-bridged Fe$^{III}$−Mn$^{III}$ assemblies; most of such systems possess ferromagnetic properties.[1e,11] The field dependence of the magnetizations was measured at fields of 0−7 T and temperatures of 2 and 5 K. The saturation magnetization at 2 K is 2.64 N$\beta$, which is smaller than the ferrimagnetic consequence of 3 N$\beta$ calculated from $M_S = g(S_{Mn} - S_{Fe})$ with $g = 2$. The low saturation magnetization is related to the Mn$^{III}$ anisotropy. A noteworthy feature is that the magnetization curve at 2 K exhibits a sigmoidal shape. This suggests that a field-induced metamagnetic transition from an antiferromagnetic state to the ferrimagnetic phase takes place. The critical field of $H_C = 6000$ G was determined from the peak position of the derivative of $M$ against $H$, as depicted in the inset of Figure 3. This metamagnetic character was manifested by the field-cooled magnetic susceptibility data (inset of Figure 2). The peaks at fields below $H_C$, 100 G and 4 kG, denote antiferromagnetic interactions between ferrimagnetic chains mediated by the extensive $\pi-\pi$ contacts of quinoline moieties. The weak interchain antiferromagnetic couplings can be readily overcome by raising the magnetic field up to 8 and 15 kG, larger that $H_C$, where no maximum in the $\chi_m(T)$ plot was visible.

In summary, we have prepared a new molecular precursor, $(PPh_4)$[Fe(mpzcq)$(CN)_3$] (**1**), a dimer, [Fe(mpzcq)$(CN)_3$][Mn(salen)$(H_2O)$]·$H_2O$ (**2**), and a one-dimensional chain, [Fe(mpzcq)$(CN)_3$][Mn(salcy)]·MeOH·MeCN (**3**). The magnetic studies reveal that antiferromagnetic couplings are operating through the Fe$^{III}$−CN−Mn$^{III}$ pathway. It is worth noting that compound **3** exhibits the field-induced metamagnetic transition, which marks the first example of the Fe−Mn chains made of *mer*-iron(III) tricyanide precursors.

**Acknowledgment.** This work was supported by a Korea Science and Engineering Foundation (KOSEF) grant funded by the Korean government (MOST) (Grant R01-2007-000-10240-0).

**Supporting Information Available:** X-ray crystallographic file in CIF format and additional synthetic, structural, and magnetic data for **1**−**3**. This material is available free of charge via the Internet at http://pubs.acs.org.

IC702001Q

(9) Yoon, J. H.; Kim, H. C.; Hong, C. S. *Inorg. Chem.* **2005**, *44*, 7714.
(10) Drillon, M.; Coronado, E.; Beltran, D.; Georges, R. *Chem. Phys.* **1983**, *79*, 449.
(11) (a) Miyasaka, H.; Ieda, H.; Matsumoto, N.; Re, N.; Crescenzi, R.; Floriani, C. *Inorg. Chem.* **1998**, *37*, 255. (b) Miyasaka, H.; Matsumoto, N.; Re, N.; Gallo, E.; Floriani, C. *Inorg. Chem.* **1997**, *36*, 670. (c) Ni, W.-W.; Ni, Z.-H.; Cui, A.-L.; Liang, X.; Kou, H.-Z. *Inorg. Chem.* **2007**, *46*, 22. (d) Ni, Z.-H.; Kou, H.-Z.; Zhang, L.-F.; Ge, C.; Cui, A.-L.; Wang, R.-J.; Li, Y.; Sato, O. *Angew. Chem., Int. Ed.* **2005**, *44*, 7742.